DOI: 10.1002/ejoc.200901174

Complexation and Dynamic Switching Properties of Fluorophore-Appended Resorcin[4]arene Cavitands

Laura D. Shirtcliff,*[a] Hai Xu,[a] and François Diederich*[a]

Keywords: Host–guest systems / Cavitands / Excimer formation / Solvent effects / Fluorescence / Conformation analysis

Fluorophore-appended resorcin[4]arene-based cavitands having pyrene (**2**) and anthracene (**3**) moieties attached to the rims were prepared by short synthetic routes. Both undergo reversible temperature- and acid- (CF_3COOD) induced *vase*→*kite* switching as evidenced by ^1H NMR spectroscopy. The ^1H NMR spectra also suggest that suitably sized solvents, such as [D_8]toluene, efficiently solvate the cavity, reducing the conformational flexibility. In [D_{12}]mesitylene, both cavitands undergo remarkably stable host-guest inclusion complexation with cycloalkanes. The larger cavity of **3** preferentially hosts cyclohexane, whereas the smaller cavity of **2** forms the most stable complex with cyclopentane. The propensity for the cavitands to facilitate π–π stacking between the chromophores was confirmed by both ^1H NMR and fluorescence spectroscopy. The interchromophoric interaction is strongly solvent-dependent: π–π stacking between the pyrene moieties of **2** is not as efficient in [D_8]toluene, as it solvates the inner cavity and prevents the two chromophores from approaching each other. Fluorescence studies revealed an unexpectedly large conformational flexibility of the cavitand structures both in the vase and kite forms, which was further confirmed by molecular dynamics simulations. Excimer formation is most preferred in [D_{12}]mesitylene when the cavities are empty, whereas efficient solvation or guest binding in the interior spaces reduces the propensity for excimer formation. The observed high conformational flexibility of the cavitands in solution explains previous differences from the behavior of related systems in the solid state. This study shows that the rigid, perfect vase and kite geometries found for bridged resorcin[4]arene cavitands in the solid state are largely a result of crystal packing effects and that the conformational flexibility of the structures in solution is rather high.

Introduction

There is extensive ongoing research focused on addressing the design, synthesis, and structural properties of dynamic supramolecular systems that can be utilized as receptors,[1] sensors,[2] molecular motors,[3] and switches.[3,4] Early developments on dynamic receptors were reported by Cram and co-workers in 1982, when the synthesis and switching properties of quinoxaline-bridged resorcin[4]arene cavitands **1** were initially investigated (Scheme 1).[5,6] These types of cavitands have been shown to reversibly switch between a container-like *vase* form (**1a**) and an extended *kite* form (**1b**) upon variation of temperature,[5b,7] pH,[8] or upon addition of Zn^{2+} ions.[9] The vase conformers are capable of incorporating a variety of smaller guest molecules, such as benzene derivatives.[10] Rebek and co-workers showed that suitable rim-functionalization not only enhances binding affinity and selectivity by deepening the cavity,[11] but also allows trapping and observation of elusive reaction intermediates in the interior space of the cavitands.[12] We recently reported that selective bridging of the resorcin[4]arene scaffold and subsequent covalent modification leads to molecular baskets with reversibly controllable guest-binding properties.[13] Upon acidification, the basket opens and guest cargo is rapidly released, where upon reneutralization of the acid with base, guest binding is completely and immediately restored.

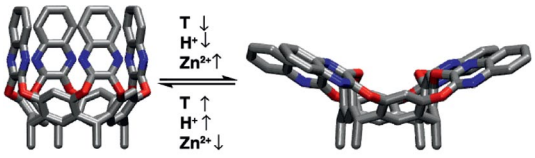

Scheme 1. *Vase*→*kite* switching in quinoxaline-bridged resorcin[4]-arene cavitands. The conversion to the *kite* form occurs reversibly upon lowering the temperature, reducing the pH, or upon addition of Zn^{2+} ions. The legs of the cavitands are omitted for clarity.

Selective functionalization of the rim of resorcin[4]arene cavitands, by attaching long rigid arms bearing terminal chromophores to two wall flaps in the *anti*-orientation, generates molecular switches featuring large, geometrically well defined contraction/expansion motions.[14–16] In the *vase* conformation, the chromophores are located in close proximity to each other, whereas in the *kite* conformation they are several nanometers apart. Different interchromophoric

[a] Laboratorium für Organische Chemie, ETH-Hönggerberg, Wolfgang-Pauli-Strasse 10, 8093 Zürich, Switzerland
E-mail: diederich@org.chem.ethz.ch

Supporting information for this article is available on the WWW under http://dx.doi.org/10.1002/ejoc.200901174.

interactions in the two states translate into different physical properties that can be utilized to quantify the switching processes. Consequently, we reported a cavitand with two oligo(phenylene ethynylene) arms terminated by a donor–acceptor BODIPY (dipyrromethene boron difluoride) dye pair.[14] In the *vase* form, the two dyes should be in close proximity (ca. 8 Å apart), whereas in the *kite* form, obtained by either acidification or a decrease in temperature, the two chromophores were predicted to be distanced by ca. 7 nm. This unprecedented, controllable expansion/contraction process was unambiguously detected by a profound difference in the fluorescence resonance energy transfer (FRET) intensity between the two states.[17] However, complete energy transfer was not seen in the *vase* form and led us towards further chromophoric investigation.

Rim functionalization of resorcin[4]arene cavitands in an *anti* orientation potentially offers a general way to investigate interchromophoric interactions at controllably switchable distances. In addition, chromophoric interactions could be modulated by the presence or type of guest complexed in the interior cavity of the *vase* form. It was also hypothesized that the appended chromophores would close off the *vase* cavity, thereby potentially enhancing binding affinity and selectivity and affecting rates for guest uptake and release. This reasoning, along with the previous results of incomplete energy transfer between the two BODIPY dyes in the *vase* form, provided the motivation for the development of the two new fluorophore-appended cavitands, dipyrene derivative **2** and dianthracene derivative **3** (Scheme 2), reported in this paper. We were particularly interested in functionalizing the rim of the cavitands with these two polycyclic aromatic hydrocarbons (PAHs), as pyrenes and anthracenes at close proximity (as in the *vase* form), are well known to undergo formation of excited dimers (excimers).[18] Additionally, two anthracenes properly oriented at close distance and orientation undergo [4+4] photodimerization. We hoped that the investigation of such processes would shed further light on the dynamics of *vase*→*kite* switching. Both excimer formation[19,20] and anthracene photodimerization[21,22] have found wide application in supramolecular systems.

Results and Discussion

Synthesis of the New Molecular Switches

Both switches **2** and **3** were constructed from resorcin[4]-arene **4**, which is bridged with two quinoxaline flaps in the *anti* orientation (Scheme 2).[23,24] The latter was transformed into aryl iodide **5**, following published protocols.[14b] Sonogashira cross-coupling of **5** with 1-ethynylpyrene (**6**)[25] afforded pyrene-appended cavitand **2** in 55% yield. For the preparation of the anthracene-cavitand **3**, 5,6-dichloropyrazine-2,3-dicarboxylic anhydride was condensed

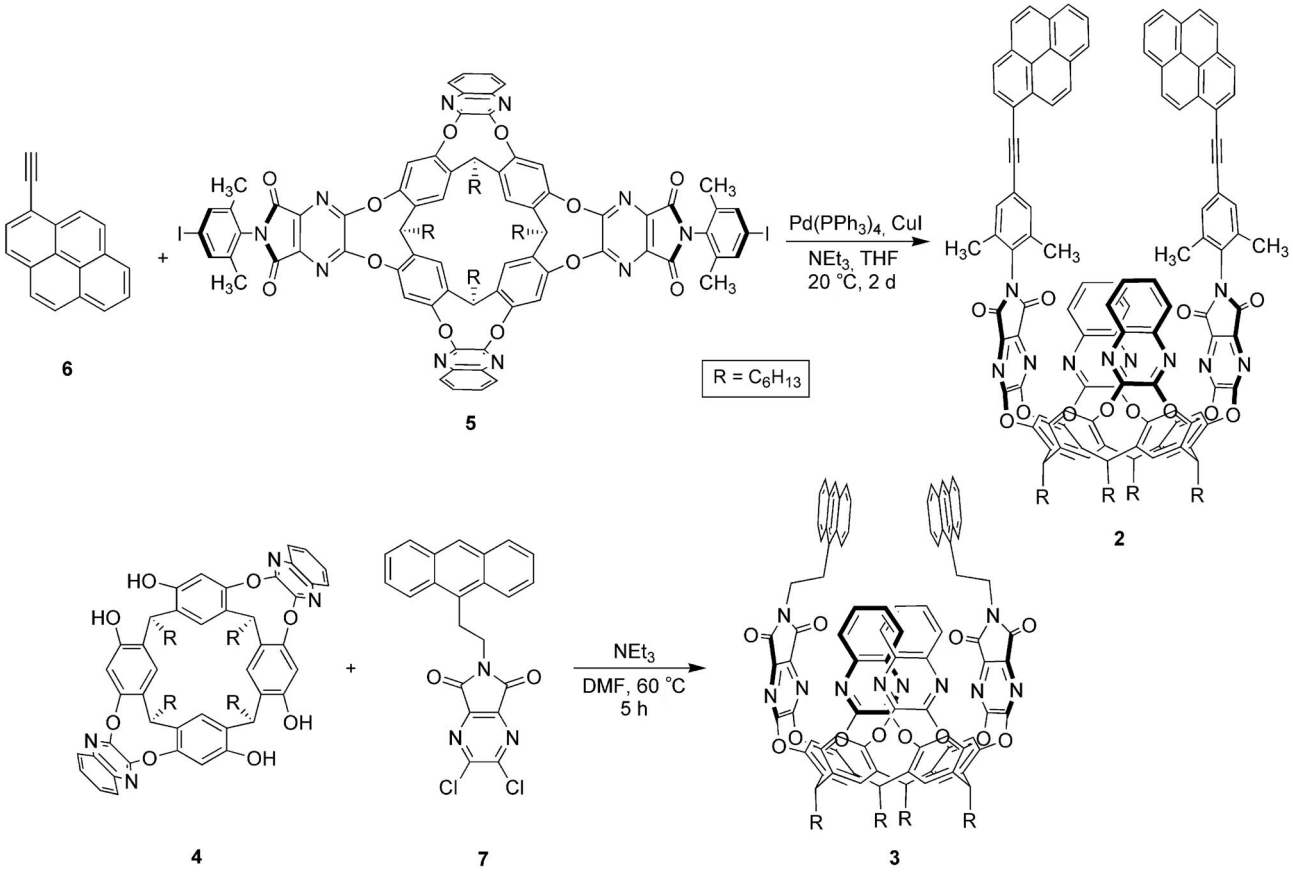

Scheme 2. Synthesis of the fluorophore-appended cavitands **2** and **3**.

with 9-(2-aminoethyl)anthracene[26] to give diazaphthalimide **7** (see Supporting Information). Subsequent bridging of **4** with **7** (NEt_3, DMF) provided target compound **3**. After chromatographic purification, it was necessary to dry **2** and **3** for 2–3 d at 10^{-8} Torr to remove any residual solvent trapped in the cavities. The structures assigned to the two cavitands are fully supported by spectroscopic data. At room temperature, both adopt the *vase* conformation as evidenced by the downfield position of the methine protons in the resorcin[4]arene bowl, around 5.5–6.1 ppm in all solvents investigated.[8b] In [D_8]toluene (300 MHz, 298 K), the two triplets for the methine protons appear at 6.08 and 5.84 (**2**) and 6.07 and 5.75 ppm (**3**), respectively (for the full spectra, see Supporting Information).

Vase→*Kite* Switching

Upon addition of CF_3COOD (0.44 M) or upon lowering the temperature to –65 °C in CD_2Cl_2, both **2** and **3** expectedly change from the *vase* to the *kite* form, as evidenced by the large upfield shifts of the methine protons in the resorcinarene macrocycle. The methine protons under both the quinoxaline and the diazaphthalimide bridges shift from about 5.6 to ca. 3.9 ppm (Figures 1 and 2). This demonstrates that all four wall flaps of the cavitand flip outwards to generate the flat *kite* geometry.[8,14] Neutralization with equimolar amounts of NEt_3 or warming the samples back to 25 °C completely reforms the *vase* conformers. However, in [D_8]toluene the switching behavior is noticeably different. Complete *vase*→*kite* conformational isomerization of **2** and **3** in this solvent requires significantly more CF_3COOD, 1.7 and 4.5 M, respectively. In addition, cooling the cavitands to –80 °C is not accompanied by *vase*→*kite* switching of either cavitand (see Supporting Information). This can be attributed to stabilization of the *vase* conformer by the aromatic solvent, as it is suitably sized to efficiently solvate the inner space.[7]

Host–Guest Complexation

As stated in the introduction, rim functionalization of bridged resorcin[4]arene cavitands deepens the cavity and can strengthen guest binding in the interior of the vase.[11] Similar results were observed with cavitands **2** and **3**: appropriate cycloalkane guests are bound much more tightly as compared to the parent system **1a** without appended flu-

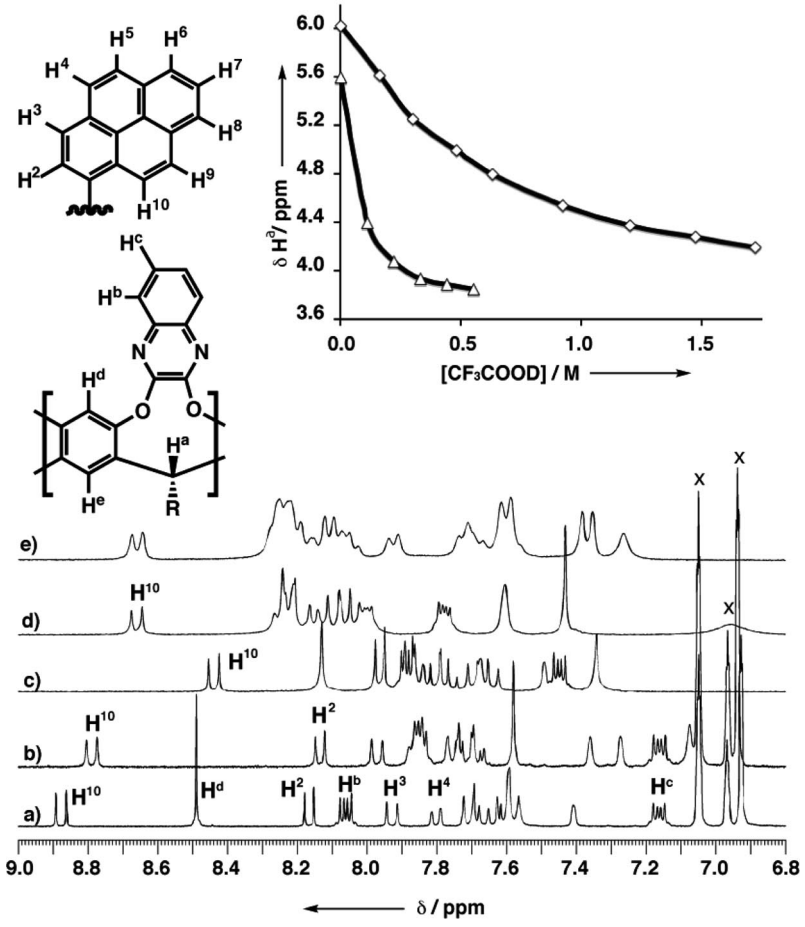

Figure 1. Bottom: Aromatic region of the ^1H NMR spectra (300 MHz) of cavitand **2** (a) in [D_8]toluene at 25 °C; (b) in [D_8]toluene at 25 °C + 1.7 M CF_3COOD; (c) in CD_2Cl_2 at 25 °C; (d) in CD_2Cl_2 at 25 °C + 0.44 M CF_3COOD; (e) in CD_2Cl_2 at –65 °C. x = solvent. Top: Chemical shifts of the methine protons H^a under the quinoxaline flaps as a function of [CF_3COOD] in [D_8]toluene (◇) and CD_2Cl_2 (Δ).

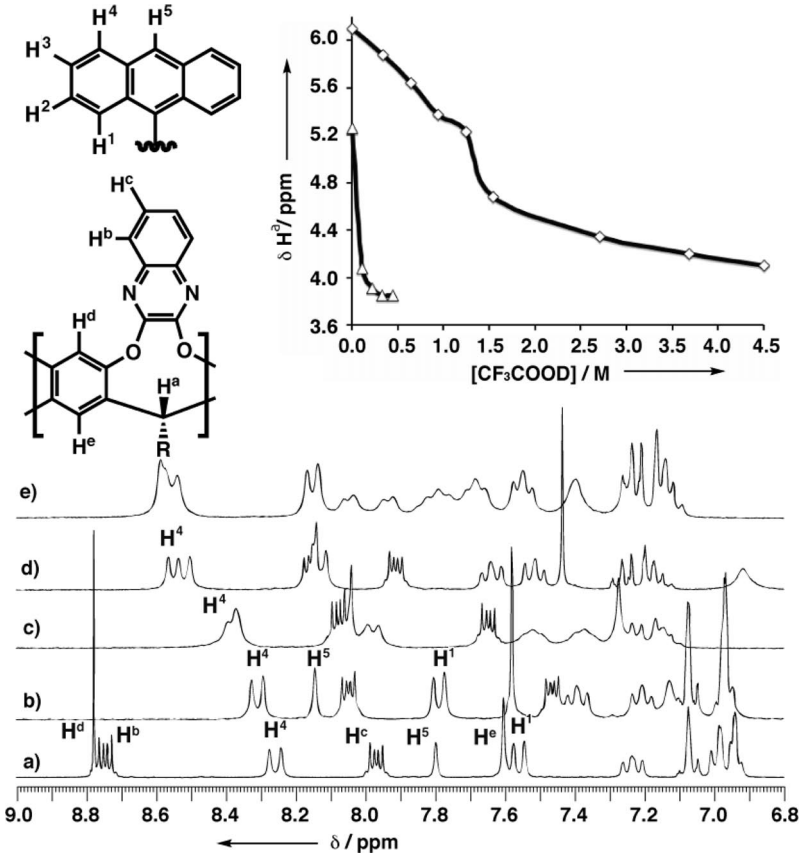

Figure 2. Bottom: aromatic region of the ^{1}H NMR spectra (300 MHz) of cavitand **3** (a) in [D_8]toluene at 25 °C; (b) in [D_8]toluene at 25 °C + 1.7 M CF_3COOD; (c) in CD_2Cl_2 at 25 °C; (d) in CD_2Cl_2 at 25 °C + 0.44 M CF_3COOD; (e) in CD_2Cl_2 at –65 °C. Top: Chemical shifts of the methine protons H^a under the quinoxaline flaps as a function of [CF_3COOD] in [D_8]toluene (◇) and CD_2Cl_2 (Δ).

orophores, where guest complexation cannot be observed by NMR spectroscopy. In cavitands **2** and **3**, host-guest exchange becomes slow enough to allow visualization on the NMR time scale at ambient temperature. This provides a convenient method for measuring the association constants, K_a, by simple integration of the resonances of free vs. bound guest. Competition experiments at 25 °C were performed in [D_{12}]mesitylene, by sequentially adding 20 equiv. of cyclopentane, cyclohexane, and cycloheptane to both cavitands. In the absence of bound solvent (or guest) in the cavity, the conformational space of the cavitands is large and different conformers interconvert (NMR time scale). Mesitylene is too large to fit into the *vase* cavity and this is reflected in the resolution of the NMR spectra: while the spectra of the cavitands in [D_8]toluene are highly resolved, those measured in [D_{12}]mesitylene are poorly resolved, showing broadened peaks. Similar behavior has been observed for molecular basket-type, capped cavitands.[13b]

Upon addition of the guests, the ^{1}H NMR spectra of both cavitands in [D_{12}]mesitylene became well resolved. Guest encapsulation was clearly apparent from the appearance of markedly upfield-shifted singlets for the bound cycloalkanes between –2.5 and –3.0 ppm, as a result of their exposure to the shielding environment of the cavity (Figure and Figure 4). At room temperature, the bound cycloalkanes are free to conformationally interconvert inside the cavitand cavity. Anthracene-appended **3** has the larger cavity as it preferentially binds cyclohexane (K_a = 222 ± 30 M^{-1}). Cyclopentane (K_a = 33 ± 0.5 M^{-1}) and cycloheptane (K_a = 19 ± 1.2 M^{-1}) are more weakly bound. This data is in agreement with the competition experiment which gives a relative ratio of the formed complexes of 0.49 (cyclo-

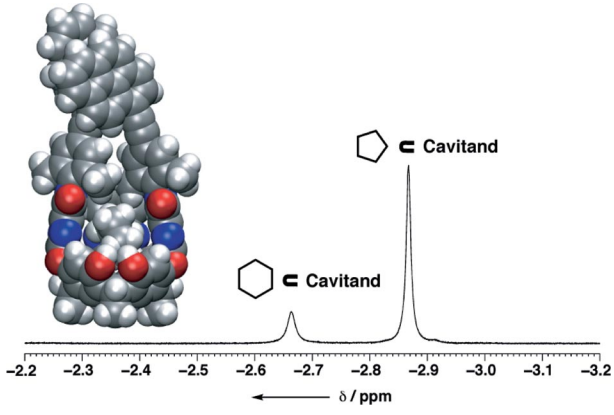

Figure 3. Partial ^{1}H NMR spectrum (500 MHz, 25 °C, [D_{12}]mesitylene) of the bound cycloalkanes in the competition experiment to determine the guest selectivity of cavitand **2**. Also shown is a computer-generated model of **2** with bound cyclopentane (Spartan PM3). The front quinoxaline flap has been removed for clarity and methyl legs are used.

pentane)/1.0 (cyclohexane)/0.23 (cycloheptane). The cavity of pyrene-appended **2** is smaller as cyclopentane (K_a = 960 ± 23 M^{-1}) is preferentially bound over cyclohexane (K_a = 487 ± 56 M^{-1}) and cycloheptane (K_a = 19 ± 0.90 M^{-1}). In the ^1H NMR spectrum of the competition experiment of **2**, there is no noticeable peak for bound cycloheptane. It is remarkable that, even though the cavitands are open at the top, they are able to undergo host-guest binding with high selectivity and with substantial association constants.

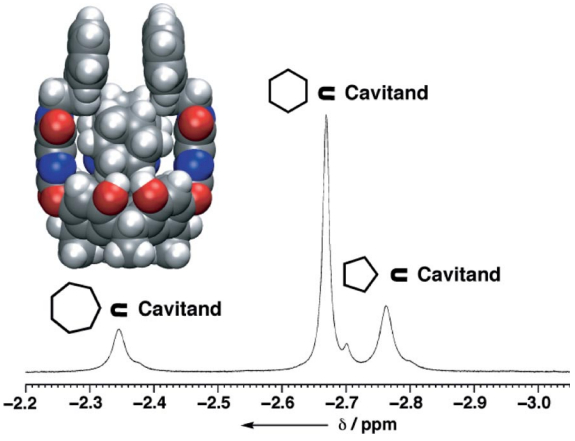

Figure 4. Partial ^1H NMR spectrum (500 MHz, 25 °C, [D_{12}]mesitylene) of the bound cycloalkanes in the competition experiment to determine the guest selectivity of cavitand **3**. Also shown is a computer-generated model of **3** with bound cyclohexane (Spartan PM3). The front quinoxaline flap has been removed for clarity and methyl legs are used.

^1H NMR Spectroscopic Investigations of Ground-State Intramolecular π–π Stacking between the Appended Fluorophores

In the expanded *kite* form of the cavitands, the pyrene chromophores in **2** and the anthracenes in **3** should not be able to undergo intramolecular π–π stacking since they are too far apart from each other. In contrast, the *vase* form should hold the chromophores at an appropriate distance to undergo intramolecular π–π stacking and we were interested in to what extent these interactions could be observed by ^1H NMR and fluorescence spectroscopy (vide supra). As a result of the anisotropy of diamagnetic ring currents, π–π stacking of polycyclic aromatic hydrocarbons leads to upfield shifts of their ^1H NMR resonances, usually in the range of $\Delta\delta \approx$ –0.2 to ca. –0.5 ppm as compared to the peak positions in the spectra of the free components. Therefore, we analyzed the chemical shifts of the anthracene and pyrene protons when the cavitand is in the *vase* form, in which intramolecular π–π stacking can occur, vs. the *kite* form, in which π–π stacking cannot (Figure 1 and 2). It can be assumed with confidence that the protonation of the two quinoxaline flaps in the *kite* form does not affect the chemical shifts of the appended chromophores but that all changes originate from differences in the interchromophoric distance.

The proton resonances for the anthracene moieties in **3** shift upfield upon changing from the *kite* to the *vase* form in both CD_2Cl_2 and [D_8]toluene. For example, the signals of H_1 and H_5 move upfield by ca. –0.2 to –0.3 ppm which provides strong evidence for intramolecular π–π stacking in the *vase* form in both solvents (Figure 2). In contrast, intramolecular interactions between the two pyrene chromophores in **2** are much more solvent-dependent. In CD_2Cl_2, π–π stacking occurs in the *vase* form as evidenced by the upfield shift from 8.63 to 8.42 ppm, measured for the resonance for H-10 upon *kite*→*vase* switching (for numbering, see Figure 1). While not all pyrene resonances are fully resolved, an overall trend for upfield shifts of all pyrene resonances in the *vase* form is apparent in the spectra recorded in this solvent. Clearly, the higher rigidity of the spacer connecting the pyrene moieties to the cavitand does not eliminate interchromophoric π–π stacking in this solvent, which can occur in two geometries, a *syn* orientation with the pyrenes in an eclipsed arrangement and an *anti*-orientation in which stacking mainly occurs only between the phenyl rings of the pyrenes that are directly attached to the alkyne spacer. In [D_8]toluene, however, there is no distinct trend for the change in chemical shifts as measured for the pyrene resonances in both cavitand geometries. Apparently, interchromophoric π–π stacking in the *vase* form of **2** is not as efficient in this solvent. We conclude that the different ability of the solvents to fill the cavity controls the resultant stacking behavior of the cavitand-attached chromophores. [D_8]Toluene strongly solvates the *vase* cavity, rigidifies the cavitand, and prevents the pyrenes from approaching each other. In contrast, CH_2Cl_2 is too small to sufficiently solvate the cavity of **2** and hence entrapped solvent does not keep the chromophores at the rim rigidly apart. The greater flexibility of the alkyl spacers in **3** obviously compensates for the effects of bound solvent and π–π stacking is observed in both solvents. Cavity solvation (or guest binding) clearly affects interchromophoric interactions at the rim of the cavitand in its *vase* form and hence cavitand conformation, and this is further exemplified by fluorescence spectroscopy date (vide infra).

Studies of Intramolecular Chromophoric Interactions by Fluorescence Spectroscopy

Monomeric pyrene and anthracene fluoresce at shorter wavelengths, and exhibit vibrational fine structure while the excimer ("excited dimer") fluorescence – a signature for π–π stacking – is significantly bathochromically shifted, broad, and featureless.[18–20] We undertook fluorescence spectroscopic investigations to further explore how solvent and guest binding by the *vase* form affects the intramolecular chromophoric interactions at the rim of the containers. Low concentration ranges were chosen to rule out competition by intermolecular excimer formation (see the spectra for reference compounds **6** and **7** in the SI).

The emission spectra of the anthracene-derived cavitand **3** ([**3**] = 2.3×10^{-5} M, λ_{exc} = 366 nm; 25 °C) were recorded in

a variety of solvents of different size (Figure 5). Monomer emission with vibrational fine structure is observed at 416 nm, whereas excimer emission appears as a bathochromically shifted, broad featureless band (e.g. at λ = 545 nm in mesitylene). In solvents that are too large to effectively solvate the *vase* cavity, such as mesitylene and *n*-pentadecane, a much higher ratio of excimer→monomer emission intensity is observed, when compared to solvents capable of solvating the interior cavity, such as cyclopentane or benzene (no excimer emission observed). The ratio of excimer to monomer is defined for our purposes as the relative fluorescence intensity at the λ_{max} of the respective type of emission, monomer and excimer. There are also pronounced solvatochromic excimer shifts observed. The excitation spectra of cavitand **3** at the respective emission maxima in mesitylene (λ_{em} = 415 [monomer] and λ_{em} = 545 [excimer]) has a slight bathochromic shift indicative of static excimer formation (see Supporting Information). Based upon the flexibilty of the cavitand we conclude that the solvatochromic nature of the excimer λ_{max} is due to varying degrees of static vs. dynamic excimer formation in the varying solvents. In the absence of cavity-solvating molecules, the cavitand walls arrange in such a manner as to minimize the amount of empty interior space and thus orient the anthracenes in a manner that allows for excimer formation. As evidenced by the solvatochromic nature of the excimer λ_{max} in solvents of similar polarity, there are also varying degrees of preassociation, resulting in static excimer formation, based upon solvent size.

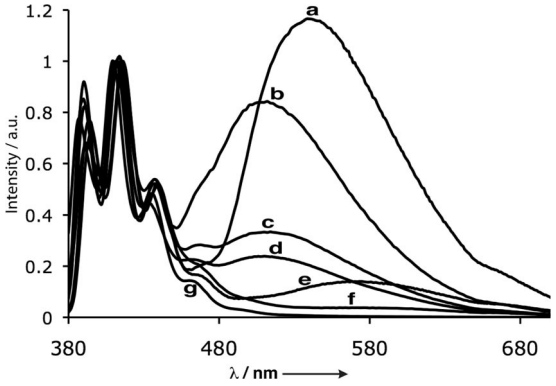

Figure 5. Emission spectra of anthracene-cavitand **3** ([**3**] = 2.3×10^{-5} M, λ_{exc} = 366 nm; emission spectra normalized at 416 nm, 25 °C) in (a) mesitylene; (b) *n*-pentadecane; (c) cyclooctane; (d) cyclopentane; (e) toluene; (f) benzene; and (g) MeOH.

Addition of CF_3COOH (2.1×10^{-1} M) to a mesitylene solution of **3** resulted in a marked decrease in excimer fluorescence intensity (Figure 6). Excimer emission, however, does not ever completely disappear, underlining the substantial conformational flexibility of the cavitand, which allows a fraction of the anthracenes to come into contact within the lifetime of the excited state. Even when the cavitand is completely converted into the *kite* conformer, on the ^{1}H NMR time scale (Figure 2), it is still capable of undergoing facile enough geometric perturbations to allow for anthracene association within the lifetime of the excited state. This underlines the hitherto poorly recognized dynamics and conformational flexibility of this cavitand system.[13b] Upon complete neutralization with NEt_3 (2.1×10^{-1} M), the initial ratio of excimer→monomer emission is not regained (Figure 6). We attribute this to the fact that, in the initial solution, the cavitand interior is completely empty and flexible allowing for efficient π–π stacking in the excited state. After acidification and neutralization, the formed triethylammonium trifluoroacetate salt along with miniscule amounts of residual TFA or NEt_3 remain, both of which can reside in the cavity. This changes the geometry of the cavitand and the ability to undergo excimer formation. To further probe this, cyclohexane (2.0×10^{-3} M), which binds well to the *vase* form of **3** (vide supra), was added to a solution of mesitylene containing the empty cavitand. This addition also decreases substantially the ratio of excimer→monomer fluorescence inten-

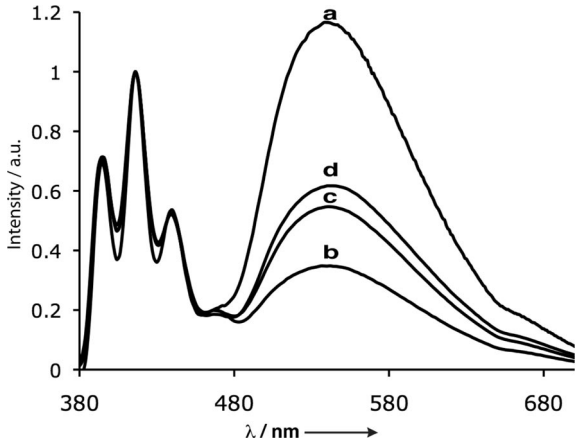

Figure 6. Emission spectra of anthracene-cavitand **3** ([**3**] = 2.3×10^{-5} M, λ_{exc} = 366 nm; emission spectra normalized at 416 nm, 25 °C) in mesitylene: (a) pure solvent; (b) after addition of 2.1×10^{-1} M CF_3COOH; (c) after addition of 2.1×10^{-1} M NEt_3 to the acidified solution; (d) in the presence of 2.1×10^{-3} M cyclohexane.

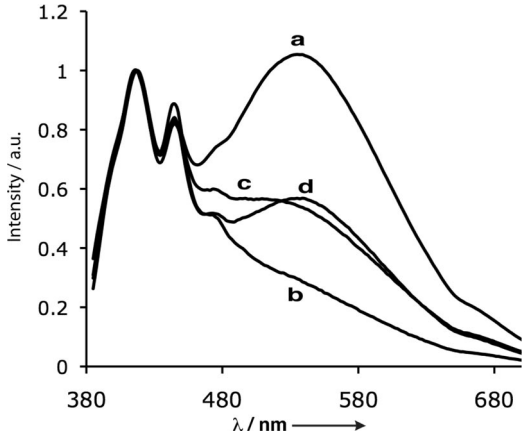

Figure 7. Emission spectra of pyrene-cavitand **2** ([**2**] = 4.5×10^{-6} M, λ_{exc} = 367 nm; emission spectra normalized at 417 nm, 25 °C) in mesitylene: (a) pure solvent; (b) after addition of 4.0×10^{-1} M CF_3COOH; (c) after addition of 4.0×10^{-1} M NEt_3 to the acidified solution; (d) in the presence of 2.0×10^{-3} M cyclopentane.

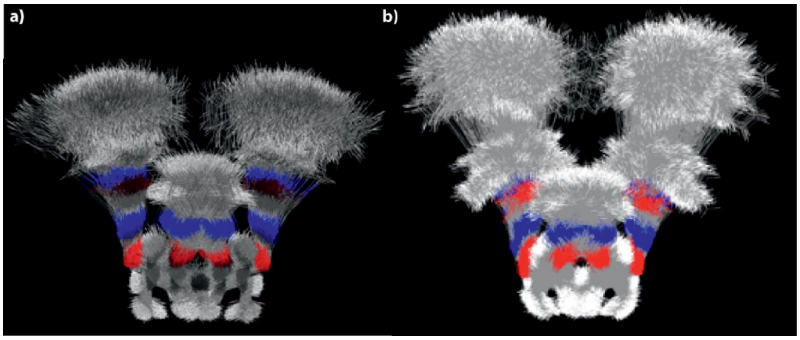

Figure 8. Overlays of 1000 structures of the *vase* forms of **2** (a) and **3** (b) sampled from molecular dynamics simulations. In both cases, the hexyl legs were substituted for methyl groups.

sities, since guest binding rigidifies the cavitand and hence hinders the two anthracene chromophores at the rim from approaching each other.

Similar results were obtained in the investigations of pyrene-appended **2** (Figure 7). In mesitylene, structured monomer emission is observed at 417 nm, whereas the maximum of the broad featureless excimer emission appears at 537 nm (trace a in Figure 7). Acid-induced switching to the *kite* form reduces the excimer fluorescence, which however never fully disappears (trace b). Re-neutralization does not regenerate the original fluorescence spectrum (trace c), and addition of cyclopentane, a good guest for **2**, to the original solution also reduces the excimer fluorescence intensity in relation to relative monomer fluorescence intensity.

From the present and a previous study[13b] it becomes now increasingly apparent that the bridged resorcin[4]arene cavitand system in both *vase* and *kite* states is much less conformationally rigid than originally thought. Only by bridging the top, as in the recently described container molecules,[13] does the interior space and positioning of the cavity walls become more precisely defined. To further explore the extent of thermal flexibility of **2** and **3**, we performed molecular dynamics simulations (1000 ps simulation time with 1.0 fs time steps, MMFF94 force field, 300 K, GB/SA solvation model for $CHCl_3$, Macromodel V. 9.5).[27] Figure 8 shows the local conformational space of cavitands **2** and **3** in the *vase* form. It is clear that there is a significant amount of conformational flexibility in the cavitands and that a majority of the time the fluorophores are not at a distance or orientation to undergo π–π stacking, in agreement with the fluorescence spectroscopic study.

Conclusions

We reported the synthesis and properties of the two novel, fluorophore-appended cavitands **2** and **3**. They both undergo reversible temperature- and acid-induced *vase-kite* switching. In $[D_{12}]$mesitylene, which does not solvate the interior cavity, the *vase* forms of both cavitands function as selective hosts with rather impressive association constants, given the open tops of the receptors. The ^{1}H NMR spectra also suggest that suitably sized aromatic solvents, such as $[D_8]$toluene, solvate the interior cavity efficiently, thereby reducing the conformational flexibility of the cavitands. The propensity for the cavitands to undergo π–π stacking between the chromophores attached to the rim is strongly solvent-dependent. ^{1}H NMR spectroscopic studies reveal that π–π stacking between the pyrene moieties of **2** is not efficient in $[D_8]$toluene, since the solvent molecules bind to the inner cavity, preventing the two chromophores from approaching each other. Both fluorescence studies and molecular dynamics simulations reveal a hitherto poorly recognized[13b] large conformational flexibility of the cavitand structure. Intramolecular excimer formation even occurs after complete switching (^{1}H NMR spectroscopy) of the cavitand into the *kite* form. The surprising observations made in the fluorescence studies mandate an extensive investigation by time-resolved spectroscopy that now has been initiated. Furthermore, some previous results are now better understood: When we reported a cavitand with two long, rigid oligo(phenylene ethynylene) arms, terminated by a donor-acceptor BODIPY (dipyrromethene boron difluoride) dye pair, we observed poor FRET efficiency in the *vase* form, despite a close proximity (ca. 8 Å apart) of the two dyes in computer models generated on the basis of X-ray crystallographic coordinates for the cavitands.[14] In view of the high conformational flexibility observed in this work, this result is no longer that surprising. While X-ray crystallographic studies usually show a perfect *vase* conformation,[5,8] with opposite walls approximately 8 Å apart, a high geometric preference and a rigid cavitand structure cannot be confirmed in solution. Presumably, the perfect *vase* form seen in the many X-ray structures is rather due to optimal crystal packing than due to high conformational rigidity. Only by bridging the rim with formation of molecular baskets[13] or by hydrogen-bonded self-assembly to give supramolecular capsular dimers[28] does the conformational space of the interior cavity of bridged resorcin[4]arene cavitands become much better defined. It is also not surprising, in view of these findings, that we were unable to detect species formed by [4+4] photodimerization of the two anthracenes in **3**, a reaction which requires a rather precise orientation of the two chromophores.

Experimental Section

Materials and General Methods: All chemicals were of reagent grade and used without further purification unless noted otherwise. All solvents for fluorescence spectroscopy were spectral grade and used without further purification. Dimethylformamide (DMF) was purchased from Fluka ($[H_2O] < 0.005\%$) and tetrahydrofuran (THF) was distilled from Na/benzophenone. All reactions were carried out under dry N_2 in flame-dried glassware following standard Schlenk techniques. Air was dried by slow passage through 25 cm Blaugel. Stationary phase for flash chromatography was silica gel 60 (Silicycle, 230–400 mesh). High-performance gel permeation chromatography (GPC) was run with a Merck–Hitachi LaChrom D-Line system, equipped with a D-7000 Interface, a L-7100 pump, a L-7200 autosampler, and a L-7400 UV-detector. Preparative separations were carried out at room temperature, and the solvent was degassed with a L-7612 degasser. HPLC-grade $CHCl_3$ was used as the mobile phase. The stationary phase was NovoGROM SDVGel 100 Å, 10 μm GPC-columns (600 × 20 mm) and the flow rate 3 mL/min. Compounds **4**,[23,24] **5**,[14b] and **6**[25] were synthesized according to published procedures. ^1H and ^{13}C NMR spectra were recorded at 298 K with a Bruker ARX 300 or a Bruker Avance DRX 500 spectrometer unless otherwise stated. ^{13}C NMR spectra are ^1H broadband-decoupled. Chemical shifts are given in ppm relative to tetramethylsilane (TMS) and were referenced to TMS or residual non-deuteriated solvent. Coupling constants J are given in Hz. High-resolution FT-MALDI ion cyclotron resonance (MALDI-ICR) mass spectra were recorded on a Ion Spec Ultima FT-ICR-MS, with 3-hydroxypyridine-2-carboxylic acid (3-HPA or DCTB mix) as the matrix. IR spectra were measured of neat samples on a Varian 800 FT-IR spectrometer and absorptions $\tilde{\nu}$ are given. Melting points were determined with a Büchi B-540 melting point apparatus in open capillary tubes and are uncorrected. UV/Vis spectroscopy (λ/nm, ε/M^{-1} cm^{-1}) was carried out with a Varian Cary 500 Scan spectrophotometer. Samples for fluorescence measurements were degassed prior to recording on an Instruments S. A. Fluorolog-3 spectrofluorimeter. Both UV/Vis and fluorescence experiments were carried out in standard 3.5 mL quartz cells with four optical windows and 10 mm path length.

(17*s*,18*s*,19*s*,20*s*)-7^6,15^6-Bis{4-[2-(1-pyrenyl)ethynyl]-2,6-dimethylphenyl}-17,18,19,20-tetrahexyl-2,4,6,8,10,12,14,16-octaoxa-3,11(2,3)-diquinoxalina-7,15(2,3)bis(5,7-dioxo-6,7-dihydro-5*H*-pyrrolo[3,4-*b*]pyrazina)-1,5,9,13(1,2,4,5)-tetrabenzenapentacyclo[11.3.1.1^{1,5}.1^{5,9}.1^{9,13}]icosaphane (2): Iodocavitand **5** (274 mg, 0.15 mmol), 1-ethynylpyrene (**6**) (169.5 mg, 0.75 mmol), $[Pd(PPh_3)_4]$ (20.8 mg, 0.0018 mmol), and CuI (3.4 mg, 0.018 mmol) were added to a N_2-charged Schlenk flask. THF (50 mL) was added and the mixture degassed by successive freeze-pump-thaw cycles. NEt_3 (0.835 mL, 6 mmol; 99.7%) was added and the mixture degassed again and left to stir at room temperature for 2 d. TLC showed that cavitand **5** was nearly completely consumed. The mixture was evaporated to dryness and purified by flash chromatography (SiO_2; MeOH/CH_2Cl_2, 1:50). The product was further purified by preparative high-performance GPC (2 x) to give cavitand **2** (167 mg, 55%) as pale yellow solid; m.p. >300 °C (dec.); R_f = 0.5 (hexane/EtOAc, 5:1); t_R(GPC): 26.70 min. ^1H NMR ([D$_8$]toluene, 300 MHz, 25 °C): δ = 0.97 (t, J = 7.1 Hz, 12 H), 1.32–1.43 (m, 16 H); 1.98 (s, 6 H), 2.00 (s, 6 H), 2.09 (q, J = 2.1 Hz, 16 H), 2.40 (m, 8 H), 5.84 (t, J = 8.1 Hz, 2 H), 6.08 (t, J = 8.1 Hz, 2 H), 7.20 (m, 4 H), 7.46 (s, 2 H), 7.62–7.77 (m, 16 H), 7.85 (d, J = 9.1 Hz, 2 H), 7.89 (d, J = 9.1 Hz, 2 H), 8.11 (m, 4 H) 8.22 (d, J = 9.1 Hz, 2 H), 8.54 (s, 4 H), 8.92 (d, J = 9.1 Hz, 2 H) ppm. ^{13}C NMR (75 MHz, $CDCl_3$, 25 °C): δ = 14.25, 18.34, 18.49, 22.85, 28.13, 29.55, 29.88, 32.06, 32.37, 32.81, 34.35, 90.50, 94.13, 117.23, 119.02, 123.97, 124.24, 124.50, 124.64, 125.33, 125.68, 125.87, 125.95, 126.25, 127.23, 128.59, 128.66, 128.97, 129.83, 130.96, 131.18, 131.63, 132.14, 132.39, 135.91, 136.32, 137.06, 137.71, 140.00, 141.74, 152.11, 152.27, 152.48, 153.27, 159.06, 161.69 ppm (46 of 52 expected resonances due to signal overlap of resonances). IR (film): $\tilde{\nu}$ = 2924, 1738, 1595, 1478, 1346, 1151, 840 cm^{-1}. UV/Vis (mesitylene): λ = 299 (129700), 369 (113000), 395 (95000) nm. MALDI-HRMS (DCTB mix): m/z calcd. for M^+, $C_{132}H_{106}N_{10}O_{12}^+$ 2022.7992; found 2022.7790.

(17*s*,18*s*,19*s*,20*s*)-7^6,15^6-Bis[2-(9-anthryl)ethyl]-17,18,19,20-tetrahexyl-2,4,6,8,10,12,14,16-octaoxa-3,11(2,3)-diquinoxalina-7,15(2,3)bis(5,7-dioxo-6,7-dihydro-5*H*-pyrrolo[3,4-*b*]pyrazina)-1,5,9,13(1,2,4,5)-tetrabenzenapentacyclo[11.3.1.1^{1,5}.1^{5,9}.1^{9,13}]icosaphane (3): Tetrol **4** (0.12 g, 0.12 mmol) and **7** (0.10 g, 0.24 mmol) were taken up in DMF (10 mL) purged with Ar (20 min) and heated to 80 °C in an oil bath until the solution became clear. NEt_3 (75 μL, 0.54 mmol) was added dropwise over 20 min, and the mixture was allowed to stir with heating for 2 h. The yellow solution was cooled to 20 °C and poured into saturated aqueous NaCl solution (200 mL) and let stir for 20 min. The bright-yellow solid was filtered, dissolved in CH_2Cl_2, and the solution passed through a short pad of SiO_2, washed with CH_2Cl_2/acetone, 25:1, and concentrated to afford the product as a bright-yellow solid which by ^1H NMR was about 90% pure. The product was additionally purified by flash chromatography (hexanes/toluene, 10:90) to afford **3** (0.16 g, 75%) as a light-yellow solid; m.p. >300 °C (dec.). ^1H NMR (300 MHz, [D$_8$]toluene, 25 °C): δ = 0.85–0.95 (m, 12 H), 1.24–1.40 (m, 32 H), 2.02–2.07 (m, 8 H), 2.24–2.36 (m, 4 H) 3.30–3.40 (m, 4 H), 5.76 (t, J = 8.1 Hz, 2 H), 6.08 (t, J = 8.1 Hz, 2 H), 7.00–7.07 (m, 4 H), 7.20 (t, J = 8.4 Hz, 4 H), 7.49 (d, J = 8.4 Hz, 4 H), 7.53 (s, 4 H), 7.71 (s, 2 H), 7.86 (m, 4 H), 8.13 (d, J = 8.4 Hz, 4 H), 8.57 (m, 4 H), 8.61 (s, 4 H) ppm. ^{13}C NMR (125 MHz, $CDCl_3$, 25 °C): δ = 14.3, 22.9, 26.6, 28.15, 28.17, 29.55, 29.59, 32.08, 32.11, 32.6, 32.8, 34.49, 34.51, 38.24, 119.0, 123.1, 123.9, 124.8, 126.2, 127.17, 127.94, 129.0, 129.4, 129.6, 131.3, 135.8, 136.9, 140.0, 142.0, 151.4, 152.41, 152.45, 153.14, 158.4, 162.4 ppm (2 aliph. resonances missing due to overlap). IR (film): $\tilde{\nu}$ = 2924, 2855 1732, 1482, 1411, 1375, 1353, 1199, 1156, 759, 726 cm^{-1}. UV/Vis (mesitylene): λ = 353 (12900), 371 (15800), 391 (14600) nm. MALDI-HRMS (3-HPA): m/z calcd. for M^+, $C_{112}H_{98}N_{10}O_{12}^+$ 1774.7366; found 1774.7306. Molecular ion cluster: 1774.7306 (29) 1775.7365 (90), 1776.7405 (100), 177.7455 (68), 178.7497 (40), 179.7598 (18). $[M + Na]^+$ cluster: 1797.7215 (32), 1798.7266 (40), 1799.7291 (28), 1800.7325 (14).

6-[2-(Anthracen-9-yl)ethyl]-2,3-dichloro-5*H*-pyrrolo[3,4-*b*]pyrazine-5,7(6*H*)-dione (7): A clean, dry pressure flask was charged with 9-(2-aminoethyl)anthracene hydrochloride[26] (0.15 g, 0.58 mmol) and 5,6-dichloropyrazine-2,3-dicarboxylic anhydride (93 mg, 0.45 mmol). Ac_2O (25 drops) was added and the flask sealed and placed in a preheated (130 °C) oil bath. After stirring for 1 h, the flask was cooled to 20 °C and H_2O (20 mL) was added and the flask sonicated for 20 min to loosen solid material. The orange solid was filtered and washed with H_2O, followed by pentane/Et_2O, 3:1. Upon drying, the orangish-yellow solid was dissolved in CH_2Cl_2 (250 mL) and passed over a short pad of SiO_2, which was washed with CH_2Cl_2/Et_2O, 25:1 (500 mL). Concentration afforded **7** (0.16 g, 84%) as a light-yellow, very sparingly soluble solid; m.p. >325 °C (dec.). ^1H NMR (300 MHz, [D$_7$]DMF): δ = 4.06–4.12 (m, 4 H), 7.59 (td, J = 8.7, 1.5 Hz, 2 H), 7.69 (td, J = 8.7, 1.5 Hz, 2 H), 8.16 (d, J = 8.7 Hz, 2 H), 8.59 (d, J = 8.7 Hz, 2 H), 8.62 (s, 1 H) ppm. ^{13}C NMR (75 MHz, [D$_7$]DMF): δ = 26.4, 38.5, 123.8, 125.3, 126.6, 127.0, 129.5, 129.7, 130.1, 131.7, 145.2, 151.7, 163.1 ppm. IR (neat): $\tilde{\nu}$ = 2971, 1789, 1726, 1392, 1305, 1225, 1215,

1125, 967, 794 cm^{-1}. MALDI-HRMS (3-HPA): *m/z* calcd. for M^+, $C_{22}H_{13}Cl_2N_3O_2^+$ 421.0385; found 421.0378 (100%), 423.0355; found 423.0344 (56%).

Supporting Information (see also the footnote on the first page of this article): UV/Vis, fluorescence, and NMR spectra of compounds **2**, **3**, and **7** are provided.

Acknowledgments

This work was supported by the Swiss National Science Foundation and the NCCR "Nanoscale Science", BaselL. D. S. thanks the U.S. National Science Foundation for an IRFP postdoctoral fellowship. We are grateful to Dr. Carlo Thilgen for his help with the nomenclature of the compounds described in this paper. We thank Jens Hornung for assistance with the analytical data.

[1] a) T. Schrader, A. D. Hamilton, *Functional Synthetic Receptors*, Wiley-VCH, Weinheim, **2005**; b) *Modern Supramolecular Chemistry: Strategies for Macrocycle Synthesis* (Eds.: F. Diederich, P. J. Stang, R. R. Tykwinski), Wiley-VCH, Weinheim, **2008**.

[2] *Optical Sensors and Switches* (Eds.: V. Ramamurthy, K. S. Schanze), Marcel Dekker, New York, **2001**.

[3] a) V. Balzani, A. Credi, F. M. Raymo, J. F. Stoddart, *Angew. Chem.* **2000**, *112*, 3484–3520; *Angew. Chem. Int. Ed.* **2000**, *39*, 3348–3391; b) E. R. Kay, D. A. Leigh, F. Zerbetto, *Angew. Chem.* **2007**, *119*, 72–196; *Angew. Chem. Int. Ed.* **2007**, *46*, 72–191; c) *Tetrahedron Symposium-in-Print 137* (Ed.: R. Taylor), *Tetrahedron* **2008**, *36*, 8231–8570; d) V. Balzani, A. Credi, M. Venturi, *Molecular Devices and Machines*, Wiley-VCH, Weinheim, **2008**.

[4] a) A. P. de Silva, H. Q. N. Gunaratne, T. Gunnlaugsson, A. J. M. Huxley, C. P. McCoy, J. T. Rademacher, T. E. Rice, *Chem. Rev.* **1997**, *97*, 1515–1566; b) M. Irie, *Chem. Rev.* **2000**, *100*, 1685–1716; c) B. L. Feringa, *Molecular Switches*, Wiley-VCH, Weinheim, **2001**.

[5] a) J. R. Moran, S. Karbach, D. J. Cram, *J. Am. Chem. Soc.* **1982**, *104*, 5826–5828; b) J. R. Moran, J. L. Ericson, E. Dalcanale, J. A. Bryant, C. B. Knobler, D. J. Cram, *J. Am. Chem. Soc.* **1991**, *113*, 5707–5714; c) D. J. Cram, H.-J. Choi, J. A. Bryant, C. B. Knobler, *J. Am. Chem. Soc.* **1992**, *114*, 7748–7765.

[6] For other early work on switchable receptors, see: a) J. Rebek Jr., J. E. Trend, R. V. Wattley, S. Chakravorti, *J. Am. Chem. Soc.* **1979**, *101*, 4333–4337; b) S. Shinkai, T. Ogawa, T. Nakaji, Y. Kusano, O. Nanabe, *Tetrahedron Lett.* **1979**, *20*, 4569–4572.

[7] P. Roncucci, L. Pirondini, C. Massera, E. Dalcanale, V. Azov, F. Diederich, *Chem. Eur. J.* **2006**, *12*, 4775–4784.

[8] a) P. J. Skinner, A. G. Cheetham, A. Beeby, V. Gramlich, F. Diederich, *Helv. Chim. Acta* **2001**, *84*, 2146–2153; b) V. A. Azov, B. Jaun, F. Diederich, *Helv. Chim. Acta* **2004**, *87*, 449–462; c) V. A. Azov, A. Beeby, M. Cacciarini, A. G. Cheetham, M. Frei, J. K. Gimzewski, V. Gramlich, B. Hecht, B. Jaun, T. Latychevskaia, A. Lieb, Y. Lill, F. Marotti, A. Schlegel, R. R. Schlittler, P. J. Skinner, P. Seiler, Y. Yamakoshi, *Adv. Funct. Mater.* **2006**, *16*, 147–156.

[9] M. Frei, F. Marotti, F. Diederich, *Chem. Commun.* **2004**, 1362–1363.

[10] a) E. Dalcanale, P. Soncini, G. Bacchilega, F. Ugozzoli, *J. Chem. Soc., Chem. Commun.* **1989**, 500–502; b) P. Soncini, S. Bonsignori, E. Dalcanale, F. Ugozzoli, *J. Org. Chem.* **1992**, *57*, 4608–4612; c) S. Zampolli, P. Betti, I. Elmi, E. Dalcanale, *Chem. Commun.* **2007**, 2790–2792.

[11] a) D. Rudkevich, G. Hilmersson, J. Rebek Jr., *J. Am. Chem. Soc.* **1998**, *120*, 12216–12225; b) B. W. Purse, S. M. Butterfield, P. Ballester, A. Shivanyuk, J. Rebek Jr., *J. Org. Chem.* **2008**, *3*, 6480–6488; c) E. Mann, J. Rebek Jr., *Tetrahedron* **2008**, *64*, 8484–8487.

[12] a) B. W. Purse, J. Rebek Jr., *Proc. Natl. Acad. Sci. USA* **2005**, *102*, 10777–10782; b) T. Iwasawa, R. J. Hooley, J. Rebek Jr., *Science* **2007**, *317*, 493–496; c) P. Restorp, J. Rebek Jr., *J. Am. Chem. Soc.* **2008**, *130*, 11850–11851.

[13] a) T. Gottschalk, B. Jaun, F. Diederich, *Angew. Chem.* **2007**, *119*, 264–268; *Angew. Chem. Int. Ed.* **2007**, *46*, 260–264; b) T. Gottschalk, P. D. Jarowski, F. Diederich, *Tetrahedron* **2008**, *64*, 8307–8317.

[14] a) V. A. Azov, A. Schlegel, F. Diederich, *Angew. Chem.* **2005**, *117*, 4711–4715; *Angew. Chem. Int. Ed.* **2005**, *44*, 4635–4638; b) V. Azov, A. Schlegel, F. Diederich, *Bull. Chem. Soc. Jpn.* **2006**, *12*, 1926–1940.

[15] M. Frei, F. Diederich, R. Tremont, T. Rodriguez, L. Echegoyen, *Helv. Chim. Acta* **2006**, *89*, 2006–2019.

[16] For examples of large contraction/expansion motions in molecular and supramolecular switches, see: a) M. Barnoiu, J.-M. Lehn, *Proc. Natl. Acad. Sci. USA* **2002**, *99*, 5201–5206; b) C. Dietrich-Buchecker, M. C. Jimenez-Molero, V. Sartor, J.-P. Sauvage, *Pure Appl. Chem.* **2003**, *75*, 1383–1393; c) ref. [3]; d) J. Wu, K. C.-F. Leung, D. Beniez, J.-Y. Han, S. J. Cantrill, L. Fang, J. F. Stoddart, *Angew. Chem.* **2008**, *120*, 7580–7584; *Angew. Chem. Int. Ed.* **2008**, *47*, 7470–7474.

[17] a) R. K. Castellano, S. L. Craig, C. Nuckolls, J. Rebek Jr., *J. Am. Chem. Soc.* **2000**, *122*, 7876–7882; b) E. S. Barrett, T. J. Dale, J. Rebek Jr., *J. Am. Chem. Soc.* **2007**, *129*, 3818–3819; c) E. S. Barrett, T. J. Dale, J. Rebek Jr., *Chem. Commun.* **2007**, 4224–4226.

[18] a) J. B. Birks, D. J. Dyson, I. H. Munro, *Proc. R. Soc. London Ser. A* **1963**, *275*, 575–588; b) I. B. Berlman, *Handbook of Fluorescence Spectra of Aromatic Molecules*, Academic Press, New York, **1965**; c) T. Förster, *Angew. Chem.* **1969**, *81*, 364–374; *Angew. Chem. Int. Ed. Engl.* **1969**, *8*, 333–343; d) J. B. Birks, *Photophysics of Aromatic Molecules*, Wiley-Intersciences, London, **1970**.

[19] For recent studies on pyrene excimers in supramolecular systems, see: a) H. Yuasa, N. Miyagawa, M. Nakatani, M. Izumi, H. Hashimoto, *Org. Biomol. Chem.* **2004**, *2*, 3548–3556; b) X. Xiao, W. Xu, D. Zhang, H. Xu, L. Liu, D. Zhu, *New J. Chem.* **2005**, *29*, 1291–1294; c) G. Venkataramana, S. Sankararaman, *Org. Lett.* **2006**, *8*, 2739–2742; d) R. Nandy, M. Subramoni, B. Varghese, S. Sankararaman, *J. Org. Chem.* **2007**, *72*, 938–944; e) M. Kumar, A. Dhir, V. Bhalla, *Eur. J. Org. Chem.* **2009**, 4534–4540; f) Z. Xu, N. J. Singh, J. Lim, J. Pan, H. A. Kim, S. Park, K. S. Kim, J. Yoon, *J. Am. Chem. Soc.* **2009**, *131*, 15528–15533.

[20] For anthracene excimers in supramolecular systems, see: a) G. Nishimura, H. Maehara, Y. Shiraishi, T. Hirai, *Chem. Eur. J.* **2008**, *14*, 259–271; b) D. C. Gonzalez, E. N. Savariar, S. Thayumanavan, *J. Am. Chem. Soc.* **2009**, *131*, 7708–7716; c) N. Jayaraj, Y. Zhao, A. Parthasarathy, M. Porel, R. S. H. Liu, V. Ramamurthy, *Langmuir* **2009**, *25*, 10575–10586.

[21] For supramolecular systems with anthracene photoswitches, see: a) J.-P. Desvergne, F. Fages, H. Bouas-Laurent, P. Marsau, *Pure Appl. Chem.* **1992**, *64*, 1231–1238; b) D. Marquis, J.-P. Desvergne, H. Bouas-Laurent, *J. Org. Chem.* **1995**, *60*, 7984–7996; c) J. H. R. Tucker, H. Bouas-Laurent, P. Marsau, S. W. Riley, J.-P. Desvergne, *Chem. Commun.* **1997**, 1165–1166.

[22] a) K. Hirose, Y. Shiba, K. Ishibashi, Y. Doi, Y. Tobe, *Chem. Eur. J.* **2008**, *14*, 3427–3433; b) C. Wang, D. Zhang, G. Zhang, J. Xiang, D. Zhu, *Chem. Eur. J.* **2008**, *14*, 5680–5686.

[23] a) V. A. Azov, P. J. Skinner, Y. Yamakoshi, P. Seiler, V. Gramlich, F. Diederich, *Helv. Chim. Acta* **2003**, *86*, 3648–3670; b) V. A. Azov, F. Diederich, Y. Lill, B. Hecht, *Helv. Chim. Acta* **2003**, *86*, 2149–2155.

[24] P. P. Castro, G. Zhao, G. A. Masangkay, C. Hernandez, L. M. Guttierrez-Tunstad, *Org. Lett.* **2004**, *6*, 333–336.

[25] G. T. Crisp, Y.-L. Jiang, *Synth. Commun.* **1998**, *28*, 2571–2576.

[26] R. A. Gardner, J.-G. Delcros, F. Konate, F. Breitbeil III, B. Martin, M. Sigman, M. Huang, O. Phanstiel IV, *J. Med. Chem.* **2004**, *47*, 6055–6069.
[27] a) *Maestro*, Version 8.0, Schrödinger LLC, New York, NY, USA, **2007**; b) *MacroModel*, Version 9.5, Schrödinger LLC, New York, NY, USA, **2007**.
[28] M. R. Ams, D. Ajami, S. L. Craig, J.-S. Yang, J. Rebek Jr., *J. Am. Chem. Soc.* **2009**, *131*, 13190–13191.

Received: October 16, 2009
Published Online: December 22, 2009

